In situ microwave assisted extraction of clove buds to isolate essential oil, polyphenols, and lignocellulosic compounds

José Gonzalez-Rivera,[a,b] *Celia Duce,*[a,b] *Beatrice Campanella,*[c] *Luca Bernazzani,*[b] *Carlo Ferrari,*[a] *Eleonora Tanzini,*[c] *Massimo Onor,*[c] *Iginio Longo,*[a] *Julian Cabrera Ruiz,*[d] *Maria Rosaria Tinè*[a,b] *and Emilia Bramanti*[c*]

[a] National Institute of Optics, (INO-CNR)–UOS Pisa, Via G. Moruzzi 1, 56124 Pisa.

[b] Department of Chemistry and Industrial Chemistry, University of Pisa, Via G. Moruzzi 13, 56124 Pisa, Italy.

[c] Institute of chemistry of organometallic compounds (ICCOM-CNR) Pisa, Via G. Moruzzi 1, 56124 Pisa, Italy.

[d] Department of Chemical Engineering, University of Guanajuato, Noria Alta s/n 36050, Guanajuato, Gto, Mexico.

* Corresponding author: e mail address bramanti@pi.iccom.cnr.it

ABSTRACT

Clove buds is a spice of relevance in food, traditional medicine, pharmaceutics and cosmetics and, among the spices, they have the highest content of total polyphenols with exceptional antiviral and antimicrobial properties. Various approaches have been reported for the isolation of essential oil from clove buds. Nonetheless, the qualitative and quantitative analysis of hydrosoluble polyphenols and solid residues simultaneously yielded during the extraction process has not been explored yet. This work is focused on the analysis of some variables effect on yield and composition of the clove buds essential oils on a green microwave assisted extraction, and the characterization and quantification of the different compounds obtained from the extraction process. A versatile coaxial dipole antenna, to directly apply the electromagnetic energy inside the extraction medium, was used to thermally activate the hydrodistillation. The composition profiles of clove buds essential oil and hydrosoluble polyphenols obtained during in-situ microwave assisted extraction (IMWAE) were analysed and quantified by head space gas chromatography mass spectrometry (HS-GC-MS) and liquid chromatography with UV/visible diode array/fluorescence detector (HPLC-DAD-FD). The solid residue was characterized by Fourier Transform Infrared (FTIR) spectroscopy and its composition in term of lignin, cellulose and hemicellulose was predicted. The green IMWAE process was compared with the conventional hydrodistillation (CH) in terms of yield and quality of isolated products. Thermogravimetry coupled to FTIR analyses of the evolved gases from the solid residue evidenced that the solid residue obtained from IMWAE of clove buds is richer in cellulose-hemicellulose than the residue obtained from CH. This can be because of microwaves that allow to remove a higher amount of phenolic compounds/lignin oligomers. The enthalpy of combustion values ($\Delta_c H$) (kJ/g) of IMWAE and CH residues were determined by calorimetric combustion and were compared with the $-\Delta_c H$ (kJ/g) values calculated using the hemicellulose, cellulose and lignin compositions predicted by partial least square chemometrics. The $\Delta_c H$ highlighted the energetic features of solid residues from IMWAE and CH for their potential uses as alternative biomass for fuel production and here firstly reported for this kind of biomass. The extraction approach here presented is environmentally friendly, highly flexible, easily controllable, time saving, and enables to break the scale-up barrier in microwave assisted industrial processes aimed to valorise aromatic herbs and eventually to exploit vegetable wasting materials. This leads to a lowering of production costs and, therefore, of the market price of isolated extracts from aromatic herbs.

Keywords: Biomass Food chemistry • Clove buds • Microwave chemistry • Polyphenols • Renewable resources

Introduction

Aromatic herbs, medicinal plants and lignocellulose biomass represent one of the most fascinating new platforms for biorefinery, which allows the extraction of an unlimited amount of different chemical compounds to be used as bioactive compounds for specific applications such as fragrances, personal care products, medicines or fuels for green energy production (Zuin et al., 2018). Most of the time, the efforts were focused on a one-target product isolation approach, such as for essential oils extraction (EOs). However, this approach leads to an increase in the costs and environmental impact of isolated products. EOs extracted from aromatic herbs are, indeed, expensive products due to their intrinsic low extraction yield and cost of their production. These complex mixtures of volatile organic compounds have been typically isolated by steam distillation (Schimdt, 2010).

Classical hydrodistillation (CH) was developed at lab scale as a simple extraction approach involving only water, herbs and energy (Rassem et al., 2016; Schimdt, 2010). Thus, the efforts to optimize this extraction process to isolate EOs were focused on the minimization of energy consumption, time and cost of the process.

Hydrodistillation has been then enhanced by the use of various energy sources and environmentally friendly extraction methods like microwave assisted extraction (MWAE) (Bagherian et al., 2011; Golmakani and Rezaei, 2008; Gonzalez-Rivera et al., 2016; Gonzalez Rivera et al., 2016; Roldán-Gutiérrez et al., 2008; Saleh et al., 2016; Tiwari, 2015), supercritical fluid extraction (SFE) (Cassiana Frohlich et al., 2019) and ultrasound-assisted extraction (Pingret et al., 2014; Roldán-Gutiérrez et al., 2008; Saleh et al., 2016). Green solvents like ionic liquids have been also tested (Ascrizzi et al., 2017). These methods have been shown suitable to produce EOs with sensorial properties similar to those obtained by CH, with the advantage in term of costs and timesaving.

The yield and chemical composition of the extracts depend on the extraction method employed for EOs isolation and the intrinsic properties of the plant (Ascrizzi et al., 2017). Considering the target of obtaining high quality and high purity EOs, significant amounts of solid residues are also produced as by-products. These solid residues are mainly condensate polyphenols or insoluble cellulosic materials (Santana-Méridas et al., 2014), which can be used as biomass precursors to obtain energy or bio-compound derivatives. In EO hydrodistillation, high amounts of condensed water (also named as herbal water or hydrosol) containing non-volatile soluble bioactive compounds with strong antioxidant properties (hydrosoluble polyphenols, proteins/enzymes, aminoacids, polysaccharides, alkaloids, alcoholic compounds and vitamins) are also produced (Petigny et al., 2014).

Polyphenols, in particular, have been found to have a strong antimicrobial and antiviral activity (Chiow et al., 2016; de Oliveira et al., 2015; Jassim and Naji, 2003; Mukhtar et al., 2008; Song et al., 2005; Zhang et al., 2020; Zhong et al., 2012). Oleuropein (Omar, 2010), for example, and its derivatives (tyrosol and hydroxytyrosol) (Yamada et al., 2009) (extracted from olive leaves, *Olea europaea*) and eugenol (extracted from cloves, *Eugenia caryophyllus L*.) (Hume, 1986) have a structure similar to the conserved amino acids of the SARS-COV-19 virus S protein involved in receptor interaction (Sivanesam and Andersen, 2019).

Hydrodistillation offer a clear opportunity to valorize by-products. This work aims to investigate the effects of several variables on yield and composition of the clove buds EO and their by-products (polyphenols and lignocellulose) using a microwave assisted hydrodistillation process with microwave energy applied *in situ* (*in situ* microwave assisted extraction, IMWAE) (Figure 1). This approach is based on the uses of a coaxial dipole antenna to directly apply the electromagnetic energy inside the extraction medium (Calinescu et al., 2017; Longo and Ricci, 2007). IMWAE has been previously successfully applied to the extraction of EO from lavender, sage, rosemary, fennel seed and clove buds (Gonzalez Rivera et al., 2016). IMWAE features a series of advantages: i) it easily provides microwave energy in a reaction vessel getting rid of the restrictions of having a defined closed metal cavity, ii) it avoids the dispersion of the radiation since all the energy generated by the magnetron is absorbed by the sample providing very high energy density and, iii) the reactor walls can be made of any material and geometry. Moreover, the reactor can be safely installed in every kind of research laboratories or industrial environments. Conventional hydrodistillation was also investigated as comparison.

Figure 1

Clove buds have been chosen in this study as ligneous, representative substrate due to its relevance in food, traditional medicine, pharmaceutics and cosmetics (Khalil et al., 2017). Cloves are the aromatic flower buds of a tree in the family *Myrtaceae, Eugenia caryophyllus,* native to the Maluku Islands in Indonesia, and mainly used as a spice. Cloves are commercially harvested primarily in India, Pakistan, Indonesia, Madagascar, Zanzibar, Sri Lanka and Tanzania. But, Indonesia and Madagascar are the main clove buds oil producer (Uddin et al., 2017). Oil is extacted from buds, leaf and stem oil. Bud oil contains 60-90% eugenol, the main component, eugenyl acetate, caryophyllene and other minor constituents (Cortés-Rojas et al., 2014). Several reports highlighted that the daily intake of cloves can help to control the glucose,

triglycerides and LDL cholesterol levels in the blood (Khan et al., 2006) and that clove buds are among the spices with the highest content of total polyphenols (Assefa et al., 2018).

The strong antimicrobial, antifungal, anti-inflammatory and antiviral activity of eugenol emerged from a number of recent studies (Marchese et al., 2017). Specifically, eugenol has shown promising antiviral activity against feline calicivirus, tomato yellow leaf curl virus, influenza A virus, herpes simplex virus type 1, herpes simplex virus 2, ebola virus, four airborne phages as well as larvicidal activity against *Aedes aegypti* (Lane et al., 2019) and references therein), anesthetic activity, inhibitory activity towards the pathogens of dental caries (Uju and Obioma, 2011), antioxidant potential, antimicrobial role (Hadidi et al., 2020), antifungal role (Munoz Castellanos et al., 2020; Wan et al., 2020), anti-inflammatory action, anti-carcinogenic effects (Nirmala et al., 2019), neuroprotective ability, hypolipidemic efficiency and anti-diabetic effectiveness (Gonzalez Rivera et al., 2016; Grumezescu et al., 2013; Lee and Shibamoto, 2001). Studies showed that eugenol inhibits the replication of influenza A virus by interfering with the ERK, p38MAPK and IKK/NF-κB signal pathways (Dai et al., 2013). Eugenol has a structure similar to conserved amino acids in the sequence of spike protein (S protein) of SARS-CoV-2, which is involved in the interaction with ACE2 receptors during infection (Sivanesam and Andersen, 2019). It is reasonable to hypothesize that the interaction of eugenol or other similar small polyphenols may interact with beta structures of S protein avoiding the attack of the virus to the host cell (Bramanti et al., 2013, 2010; Sgarbossa et al., 2013). Eugenol is generally recognized as a safe and non-mutagenic compound by World Health Organization ("TOXNET. Toxycologycal data network: Eugenol," n.d.). Novel application of clove EO includes its use as a green monomer to produce polymers (Deng et al., 2015).

Clove bud polyphenols have a powerful antimicrobial and antiviral activity (Chiow et al., 2016; de Oliveira et al., 2015; Jassim and Naji, 2003; Mukhtar et al., 2008; Song et al., 2005; Zhang et al., 2020; Zhong et al., 2012). Among these, quercetin has been found have a potential role against coronavirus disease 2019 (COVID-19) (Derosa et al., 2020). In several applications polyphenols have been used to treat materials in order to give them antiviral properties (Catel-Ferreira et al., 2015; Kazuo and Yoshikatzu, 1997).

In view of the properties mentioned above, in this work IMWAE has been applied to clove buds (i) as representative, complex, ligneous matrix, (ii) in order to chemically characterize not only EO, but also residual condensed water and solid residue after IMWAE and CH. While many extraction approaches have been addressed only to optimize the yield of clove EOs, few information are reported in the literature on the chemical composition of by-products. EO composition has been assessed using headspace gas chromatography mass spectrometry (HS-GC-MS). The polyphenolic profile of water extracts has been assessed by liquid chromatography with UV/visible diode array and fluorescence detector (HPLC-DAD-

FD). The solid residue obtained after IMWAE and CH has been characterized by thermogravimetric analysis coupled to FTIR (TGA-FTIR), ATR-FTIR and by calorimetric combustion. TGA-FTIR has allowed us to investigate the thermal behaviour and the composition of the gases evolved during the thermal decomposition of the solid residues after both IMWAE and CH of clove buds. FTIR spectroscopy coupled to partial least squares (PLS) analysis has allowed us to quantify the lignin, cellulose and hemicellulose content of solid residue by applying a chemometric method previously developed (Chen et al., 2010). Enthalpy of combustion values ($\Delta_c H$) was also calculated based on the calorimetric combustion of IMWAE and CH. This information, which is reported here for the first time, is potentially useful for the alternative uses of these solid residues as fuels for energy production.

Experimental

Materials

Dry clove buds (Indonesia) were purchased from a local market. Phloretin, ellagic acid, resveratrol, chlorogenic acid, cyanin chloride, coumarin, quercetin, tannic acid, resorcinol, pyrocatechol, pyrogallol, (−)-epicatechin, gallic acid, (−)-epigallocatechin gallate, rosmarinic acid, trans-ferulic acid, caffeic acid, 1,3,5-trihydroxybenzene dehydrate, salicylic acid, acetylsalicylic acid, (+)-abscisic acid, vanillin, pinoresinol, (+)-catechin and eugenol were HPLC analytical standards purchased from Merck (Milan, Italy). Tyrosol, hydroxytyrosol, oleuropein, syringic acid, luteolin and apigenin were purchased from Extrasynthese (Cedex, France). Deionized water obtained with a Milli-Q system (Purelab Pro + Purelab Classic, Millipore, USA) was used as a solvent for all the extractions. Ethanol (EtOH for HPLC, ≥99,8%, Fluka), methanol (MeOH for HPLC ≥99%, Merck), dimethyl sulfoxide (DMSO for GC ≥99,5%, Merck), sodium hydroxide (NaOH 0.1 M, Merck) and formic acid (≈98%, Fluka) were used as solvents for the preparation of standards solution of polyphenols.

In situ microwave assisted extraction (IMWAE)

The IMWAE apparatus, experimental set-up and extraction procedure are described as follow based on our previous works with slight modifications (Gonzalez Rivera et al., 2016). Dry clove buds were ground to a fine powder using a laboratory blender. A weighted amount (5, 10 or 20 g) of grounded clove buds was mixed with 200 mL of deionized water and the aqueous substrate dispersion was loaded into a 350 mL flask vessel. The vessel was wrapped by a metallic grid to prevent the emission of MW irradiation out of the

reaction medium and to ensure safe operating conditions. MW energy was applied by means of a coaxial dipole antenna immersed into the extraction medium, protected by a glass tube. The extraction medium was heated in the MW assisted device, for 10 min using 150 W of MW power while continuously stirring the mixture at 250 rpm. The source of microwave was a magnetron oscillator equipped with forward and reflected power indicators (SAIREM, Mod. GMP 03 K/SM, up to 300 W of continuous MW irradiation power at a frequency of 2.45 GHz). Once the hydrodistillation had started, the power was kept at 150 W for 90 min under steady state conditions. The extraction time has been selected based on literature reports and previous published data of clove bud extraction by coaxial microwave assisted hydrodistillation (Gonzalez Rivera et al., 2016). After completion of the extraction process, the EO was collected, decanted, dried and weighed. The condensed water remained in the flask vessel was separated from the solid clove bud residue by 12 min centrifugation at 5000 RPM. EO and condensed water were stored at 4 °C and -20 °C, respectively, in dark containers for further HS-GC-MS and HPLC-DAD-FD characterization. The condensed water after extraction, also known as hydrosol, or herbal water corresponds to the total volume of water used for the hydrodistillation. The concentration of water-soluble polyphenols hence corresponds to the total amount of water used for the extraction. The solid residues were dried at 60 °C overnight before FTIR and TGA-FTIR. Deionized water has been employed in this work for analytical purposes of the products. For the scale up in industrial processes any type of water can be employed depending on the subsequent use of the products.

EO extraction by conventional hydrodistillation (CH)

Hydrodistillation of clove buds using conventional heating was also performed for comparison. Briefly, 5 g of ground clove buds were loaded together with 200 mL of deionized water in a typical Clevenger extractor. The extraction was thermally activated using a standard electric mantle operating at 250 W. Both IMWAE and CH processes have been operated at 100°C. This detail has been added in the experimental.

HPLC-DAD-FD analysis

Condensed water extracts were analyzed using HPLC-DAD-FD system. An HPLC gradient pump (P4000, ThermoFinnigan) was coupled with a vacuum membrane degasser (SCM1000, ThermoFinnigan), an AS3000 autosampler (ThermoFinnigan), a UV6000 diode array detector and a FL3000 fluorescence detector (ThermoFinnigan). Separations of polyphenols were carried out using a reversed-phase HPLC

column C18 Spherisorb S5 ODS2 (Waters, 250 mm x 4 mm, 5 µm). Column temperature was set at 40 °C and injection volume was 20 µL.

Mobile phases for the determination of polyphenols in standard solutions and condensate water samples was 5% methanol–0.1% formic acid in water (eluent A) and 95% methanol-0.1% formic acid in water (eluent B). The gradient was as follows: 0–5 min, 100% A; 5–45 min, linear gradient up to 100% B; 45–55 min 100% B; 55–57 min, linear gradient up to 100% A. Post-run time was 15 min. Elution was performed at a solvent flow rate of 0.8 mL min−1. Table S1 summarized the retention time (t_R), solvent used for stock solution preparation and spectra information (UV absorbance (λ_{max}) and fluorescence ($\lambda_{excitation}$/ $\lambda_{emission}$)) of 31 polyphenols standards separated using the above conditions.

ChromQuest™ 4.2 Chromatography Data System was used to carry out HPLC-DAD/FD control, data acquisition and data analysis.

Headspace gas chromatography/ mass spectroscopy (HS-GC-MS)

Clove bud essential oils were analysed by HS-GC-MS. The analysis was carried out using an Agilent 6850 gas chromatograph coupled with an Agilent 5975c mass spectrometer. An Agilent GC Sampler 80 was employed for HS sampling. The vials were incubated at 80 °C for 15 min. The chromatographic separation was carried out on a J&W DB-WAX Ultra Inert column, (60 m × 0.25 mm, 0.5 µm film thickness) supplied by Agilent Technologies (USA). Helium 5.6 IP was used as a carrier gas at constant flow of 1 mL/min. The oven temperature program was as follows: 40 °C for 5 min, 19 °C/min up to 230 °C. The total runtime was 58 min. The temperature of the transfer line and ion source was set at 240 and 250 °C, respectively.

ATR-FTIR spectroscopy analysis

Infrared spectra were recorded by using a Perkin-Elmer Spectrum One FTIR Spectrophotometer, equipped with a universal attenuated total reflectance (ATR) accessory and a triglycine sulfate TGS detector. Measurements were performed in attenuated total reflectance (ATR) mode after background acquisition. For each sample, 32 scans were recorded, averaged and Fourier-transformed to produce a spectrum with a nominal resolution of 4 cm^{-1}.

Thermogravimetric- Fourier-transform infrared spectroscopy analysis (TG-FTIR)

The thermogravimetric experiments were performed using a TA Instruments Thermobalance model Q5000IR equipped with an FTIR Agilent Technologies spectrophotometer model Cary 640 for Evolved Gas Analysis (EGA). TG-FTIR measurements were performed using Pt crucibles at a rate of 20 °C/min, from 30 °C to 900 °C under air or nitrogen flow (80 mL/min). The amount of sample in each measurement varied between 10 and 15 mg. Mass calibration was performed using certified mass standards, in the 0–100 mg range, supplied by TA Instruments. The temperature calibration was based on the Curie Point of paramagnetic metals. TG-FTIR measurements were performed in the range 600–4000 cm^{-1} with a 4 cm^{-1} width slit. To reduce the strong background absorption from water and carbon dioxide present in the atmosphere in the TG-FTIR spectra, the optical bench was usually purged with nitrogen. In addition, a background spectrum was taken before the beginning of each analysis in order to zero the signal in the gas cell and to eliminate any contribution from ambient water and carbon dioxide.

Combustion calorimetry

Combustion of biomass samples was carried out by a home-made bomb calorimeter. A standard stainless-steel bomb (volume = 375 ml) is placed in a bath with 2200 ml of water, equipped with a stirring system and a temperature probe (thermistor). The bath is lodged in an isoperibol calorimeter. The calorimetric curves are acquired by a personal computer and corrected to account for the heat losses through the calorimetric wall. The calorimeter was previously calibrated by benzoic acid certified standard. One gram of sample was pressed to form a pellet and placed in a crucible with about 0.5 g of hexadecane. An iron wire was then immersed in the hexadecane and connected to electrical terminals. Then, about 0.5 ml of water where placed in the bottom of the bomb in order to saturate the vapor phase of water and get the higher calorific value of the sample. Finally, the bomb was closed and pressurized with oxygen (99.9%, 25 bar) after flushing for about 30 seconds, placed in the calorimeter and the sample was ignited. The ΔU value was obtained for each experiment from the thermal effect, corrected for the heat losses. The blank contribution due to the combustion of the ignition wire and hexadecane was subtracted. The experiments were carried out at 25 ± 0.1 °C. The enthalpy of combustion can be obtained by Eq. (1):

$$\Delta_c H(p,T) = \Delta_c U(p,T) + \Delta\nu_g RT \qquad (1)$$

where $\Delta\nu_g$ is the variation of number of moles of gaseous species due to the combustion. However, since $\Delta\nu_g = 0$ for both cellulose and hemicellulose, only the contribution due to lignin combustion should be

considered. Considering that the molar fraction of lignin in the biomasses here analysed is between 0.15 and 0.26, the correction term to calculate $\Delta_c H$ from $\Delta_c U$ is between -0.003 and -0.005 kJ g^{-1}, which is within the experimental error. The correction for pressure value, $p \neq 1$ bar, is neglectable, as well. The overall uncertainty on the $\Delta_c H$ values is within ±2% (N=3).

Results and discussion

Clove buds essential oil yield and composition

Clove buds are well known attractive substrate due to their high EO content and low cost. The maximum amount of clove EO that can be extracted depends on their geographical origin of production, on the part of the plant used for their extraction (leaves, buds or mixture thereof), on the pre-extraction treatment and the extraction method employed. Figure 2 (a) shows the yield percent of clove buds EO isolated by IMWAE using different liquid to solid ratio (L/S_{ratio}=10, 20 and 40) and fixed MW extraction conditions (reflux of water using 150 W of MW at 2.54 GHz).

High EO extraction yields ranging from 5.5±0.8 up to 16±1.5% were obtained after 90 min of IMWAE. The EO yield % strongly depends on the liquid to solid ratio, achieving the highest value at the highest ratio explored. Figure 2 shows also the clove buds EO yield % obtained by CH as comparison. The extraction of EO by CH was performed using the best liquid to solid ratio value explored (L/S_{ratio}=40) used for the IMWAE. Under such conditions, CH yielded lower EO amount (7.8±0.8% wt) even if the extraction time used was more than 30% longer (120 min). Thus, IMWAE confirmed its advantages as faster and greener approach than CH, yielding higher amount of EO, as previously observed (Gonzalez Rivera et al., 2016).

Figure 2

Table 1 summarizes the literature reports concerning the isolation of clove buds extracts by different approaches. EO yield values (widely ranging from 2.4 up to 41.8%) depend on both the extraction conditions (time, L/S_{ratio} and solvent) and the extraction approach used. The comparison between the different approaches (to maximize the yield %) is difficult since the clove bud cultivar and geographical origin are also important factors.

As general remarks, according to Table 1 standard, conventional hydrodistillations (Chin this work) and steam distillation (SD) methods using water as solvent and the longest extraction times (from 120 to 360 min and from 240 to 600 min for CH and SD, respectively) reach yields below 10% (wt) if the L/Sratio is below 1:10 (w/w) (Gonzalez Rivera et al., 2016)(Leon-méndez et al., 2018) (Guan et al., 2007) and up to 20% (wt) if the L/Sratio increases up to 1:20 (Clifford et al., 1999) (Kapadiya et al., 2018). MW assisted extraction methods (IMWAE, MAE, MASE and MWHD) slightly increase the EO yields strongly decreasing the extraction times (from 30 to 120 min) (Gonzalez Rivera et al., 2016) (Kapadiya et al., 2018) (Golmakani et al., 2017)(Leon-méndez et al., 2018).

The highest yield (up to 41.8%) (Guan et al., 2007; Yang et al., 2014) was obtained using Soxhlet extraction (SE) and ethanol for 360 min. These features and the need of an additional step to separate the solvent from EO, make solvent approach unfavorable for environmental and economic reasons. Supercritical fluid extraction (SFE) has become a popular approach for treatment of clove buds, achieving high yields (Clifford et al., 1999; Guan et al., 2007; Reverchon and Marrone, 1997; Scopel et al., 2014; Yang et al., 2014). However, high pressure processing (from 100 up to 200 bar) and long extraction times (from 110 up to 330 min) can considerable influence the cost of EO production, beside the intrinsic concerns in the safety of the process due to high pressures involved.

Ultrasound assisted extraction (UAE) is a green approach and high EO yields (up to 41%) are obtained in short extraction time (45 min) (Alexandru et al., 2013; Tekin et al., 2015). The EO yields enhancement using UAE is related to the US negative pressure cavitation effects. The cell membranes of the substrate are disrupted by the hammer-like action of the produced solvent jets. However, this approach still uses organic solvents or water-organic solvent mixtures that require an additional step of separation of the organic solvent.

The IMWAE proposed in this work presents relative short extraction times (90 min) at atmospheric pressure, it uses only water as solvent, and it gives yields up to 16% EO without additional purification steps. Further benefits of IMWAE deal with an easy scale up, flexible technology, environmentally friendly approach, safe operations, and low cost.

Figure 2 (b) shows the chemical composition, expressed as percentage, of EO isolated from clove buds using IMWAE and CH, as comparison. Five compounds were identified by HS-GC-MS analysis, corresponding to the full EO characterization. Eugenol was the main compound (48.9±2.5 %) followed by β-caryophyllene (42.8±2.1 %). These two compounds account for more than 90% of EO composition. Other identified compounds were α-caryophyllene (3.7±0.2 %), α-cubebene (2.3±0.1 %) and α-copaene (2.2±0.1 %). The chemical composition of clove buds EO isolated through IMWAE or CH resulted statistically indistinguishable.

Table 1 also enlists the main compounds of clove EO extracted using clove buds from different geographical sources, different approaches and extraction conditions. Despite the many diverse factors involved during extraction, eugenol was the most abundant compound in all cases, with the exception of UAE procedure (Alexandru et al., 2013) where α-humulene was reported as the main compound obtained from various clove buds from China, India and Madagascar. β-caryophyllene and eugenyl acetate were also observed in clove buds EO almost in all cases, particularly in EO from clove buds from China and India (Table 1). Their composition, however, is more linked to the cultivar of buds used. EO extracted in this work from Indonesia clove buds have 42.8±2.1 % of β-caryophyllene while eugenyl acetate was not detected.

β-caryophyllene has been recently widely investigated due to its potential properties in biomedical applications as anti-carcinogenic (Fidyt et al., 2016) and organoprotective agent like the phytocannabinoids (Al-taee et al., 2019).

Table 1

Quantitative and qualitative analysis of hydrosoluble polyphenols

Figure 3 shows the HPLC-DAD (a) and FD chromatograms (b) of condensed water obtained after EO extraction by IMWAE and CH using a L/S_{ratio}=40 and, 90 min and 120 min of extraction time, respectively. Nine different main polyphenols were identified by the comparison of both UV absorbance/fluorescence spectra and retention time (t_R) of their corresponding analytical standards. To this purpose, an HPLC-DAD-FD method using 31 analytical standards was developed; eluent conditions, instrumentation, and polyphenols used in this work (including t_R and spectra information, λ_{max}) are fully described at the experimental section and listed in Table S1 of ESI.

Gallic acid (t_R =12.2min), chlorogenic acid (t_R=22.6min) and eugenol (t_R=32.5min) were detected in the absorbance chromatogram at 280 nm (Figure 3 (a)). Tyrosol (t_R=19.3 min), catechin (t_R=20.4 min), (-)epicatechin (t_R=23.4 min), acetylsalycilic acid (t_R=27.5 min) oleuropein (t_R=30.2 min), and pinoresinol (t_R= 32.5min) were identified using the fluorescence detector (Figure 3 (b)). Condensed water from CH showed a similar phenolic profile.

The condensed water, from IMWAE and CH, of clove buds is, thus, rich of bioactive compounds with well known, strong antioxidant properties (Pandey and Rizvi, 2009).

Among the different polyphenols detected, gallic acid, chlorogenic acid and eugenol were identified as the main compounds and their quantification is shown in Figure 3 (c) and 3 (d).

354

355 **Figure 3**

356

357 In the condensed water the composition of polyphenols showed small differences with respect to the
358 different extraction approaches employed (Figure 3 (c)). IMWAE yielded water extracts with almost one-
359 third of eugenol than that obtained from CH. Since eugenol is the main compound of clove buds EO, and
360 the EO yield is higher using IMWAE, the residual lower concentration in the aqueous extracts can be
361 explained with its more effective MW-mediated extraction and separation from the aqueous extraction
362 mixture. This result agrees with the higher EO yield obtained by IMWAE (Figure 2 (a)). The concentration
363 of gallic acid in the condensed water obtained using microwaves (10.4 mg/g) was slightly lower than in
364 that from CH (13.9 mg/g). The amount of chlorogenic acid in the condensed water from IMWAE (1.9
365 mg/g) was comparable with that from CH (1.7 mg/g).
366 Figure 3 (d) shows the composition of hydrosoluble polyphenols extracted using different L/S_{ratio} by
367 IMWAE. In agreement with the increase of EO yield as the L/S_{ratio} increases, the concentration of eugenol
368 in the condensed water decreased as the L/S_{ratio} increased: eugenol was, indeed, distillated from the aqueous
369 phase to the EO organic phase. However, in the cases of gallic acid and chlorogenic acid, the composition
370 in the condensed water seems to have a maximum at $L/S_{ratio}=20$. The L/S_{ratio} during the IMWAE is an
371 important factor to be controlled when the aim of the hydrodistillation is both the EO production and/or the
372 polyphenols valorization.
373 Few works reported in the literature deal with the characterization and quantification of polyphenols
374 extracted from clove buds. Adefegha et al. reported the phenolic profile of the water obtained after cooking
375 clove buds and they quantified gallic acid, catechin, chlorogenic acid, caffeic acid, ellagic acid, rutin,
376 quercitrin, quercetin, kaempferol, and luteolin by HPLC-DAD analysis (Adefegha et al., 2016). The use
377 of solvents like methanol has been also investigated for the specific extraction of polyphenols from clove
378 buds (Dua et al., 2015). Gallic acid, eugenol, quercetin and tocopherol were identified in the methanol-
379 water (80:20 v/v) extracts after 4 h of extraction at room temperature (Dua et al., 2015). The total amount
380 of polyphenols extracted was enhanced by the use of methanol.
381 The analysis of hydrosoluble polyphenols isolated in the condensed water after EO clove bud extraction
382 has been limited to the total phenolic content assay (TPC) (Table 1). In this work, a qualitative and
383 quantitative analysis of the condensed water obtained during clove buds EO isolation by both IMWAE and
384 CH has been reported for the first time.

In summary, the amount of hydrosoluble polyphenols, with strong antioxidant properties, found in the condensed water after the extraction of EO from clove buds, is significant and it opens new opportunities for condensed water valorisation.

FTIR-PLS analysis and thermal behavior of lignocellulosic residue

The solid residues remaining after the treatment of aromatic herbs aimed to extract EO represent the highest mass of by-products after HD and it has been usually managed as waste, typically burned for energy production (Kapadiya et al., 2018). This practice, however, is not efficient because of the high moisture content of the solid residues, which leads to high costs of waste disposal. This type of solid residue is rich of biopolymers like cellulose, lignin, hemicellulose, which represent a low-cost feedstock for biorefining. The depolymerization of lignocellulosic material into several feedstock chemicals such as glucose, furfurals, levulinic acid and other compounds, is clearly a greener alternative (González-Rivera et al., 2014). However, its potential uses, as renewable feedstock, have been limited due to the scarcely available information of its chemical composition.

Fourier Transform Infrared spectroscopy, thermogravimetric analysis and calorimetric combustion were carried out in this work in order to characterize the solid residue after the IMWAE and CH. Figure 4 (a) shows the FTIR spectra of raw dry clove buds and the corresponding extracted EO. The two spectra have similar structural features due to the high amount of EO contained in the raw clove buds. The main peaks observed match with the spectral profile of eugenol (OH stretching at 3516 cm^{-1}, symmetric and asymmetric stretching of methylene and methyl groups at 2920 and 2853 cm^{-1}, CO bending at 1230 cm^{-1}, and C-C stretching vibrations in the phenyl ring at 1640 cm^{-1}, 1514 cm^{-1} and 1430 cm^{-1}), which is the main compound in clove buds EO. Figure 4 (b) shows the FTIR spectra of the solid residues in the fingerprint region (1900-800 cm^{-1}) after the IMWAE and CH. The intensity of the peaks corresponding to eugenol was strongly reduced and two main peaks at 1618 and 1029 cm^{-1} (C=O and C-O stretching vibrations of cellulose and lignin) were observed. The solid residues of clove buds after both extraction processes showed the characteristics of softwoods due to the peaks at 1316 cm^{-1} (due to the condensation of guaiacyl unit and syringyl unit, syringyl unit and CH_2 bending stretching) (Jiao et al., 2017), 1272 cm^{-1} (guaiacyl ring breathing and C=O stretching), 1160 cm^{-1} (C-O-C stretching in pyranose rings, C=O stretching in aliphatic groups) and 894 cm^{-1} (due to cellulose P-chains and C–H stretching out of plane of aromatic ring) (Chen et al., 2010).

Figure 4

The composition of cellulose, hemicellulose and lignin in the solid residue after EO extraction and raw clove buds were predicted using a partial least square (PLS) model previously reported for the determination of the chemical composition of hard and softwood samples (Chen et al., 2010). The PLS model was reconstructed using the FTIR spectra of the wood samples in the region of 1900-800 cm^{-1} (which contains the fingerprint of wood components). The first derivative of the normalized FTIR spectra were used as the X matrix and the chemical composition of lignin, cellulose and hemicellulose (determined by Van Soest analysis) as the Y matrix (Chen et al., 2010). The model was developed using JMP software and 7 principal components that explain the 98% of the variance in the X matrix and 98.8% of the variance in the Y matrix (Chen et al., 2010). The prediction of the clove buds solid samples was then performed loading their first derivative of the normalized FTIR spectra (Figure 5 (a)) into X matrix of the model and the cross-validation technique was applied. Figure 5 (b) reports the comparison of the predicted chemical composition in terms of cellulose, hemicellulose and lignin in raw clove buds and in the dry solid residue after IMWAE or CH EO extraction.

Figure 5

The PLS predicted chemical composition of raw clove buds indicate that hemicellulose (26 %), cellulose (19 %) and lignin (37%) represent about 80%. The mass balance is reached considering about 15.4 - 16.1% volatile compounds (which include EO and 4-5% water determined by TGA under nitrogen flow (step 1 of weight loss in Table 3 below) and 5% inorganic materials (determined as ash by TGA under oxygen flow).

The PLS predicted chemical composition of dry solid residue after IMWAE or CH EO extraction (Table 2) evidenced that the three different components account for 78 and 80 % in the mass balance, respectively. Considering that about 6% is due to volatile compounds determined by TGA under nitrogen flow (step 1 in Table 3 below) and less than 4% is due to inorganic material in both, it can be hypothesized that the missing part to the mass balance (about 12% and 10% in IMWAE and CH dry residue, respectively) is due to a partial loss of lignin (Kang et al., 2013; Toledano et al., 2014).

Table 2

Interestingly, lignin apparently decreases, and cellulose apparently increases in dry residues depending on the thermal treatment that characterizes the respective extraction method, and this is more enhanced in solid residues after IMWAE extraction (Table 2). This result is not surprising considering that microwaves may promote a partial degradation of lignin or other wood components (e.g. hemicellulose or cellulose), suggesting a higher interaction of phenolic compounds with microwaves, thus giving higher EO yields. In the specific case, the apparent increase of cellulose may be due to a bias of the PLS model based on the van Soest extraction of whole, untreated woods (Chen et al., 2010). Following the hypothesis above, the insoluble part derived from lignin degradation may interfere with the quantitation of cellulose. Hemicellulose percentage in the solid residue from CH (24 %) was comparable with that contained in raw clove buds (25 %) and slightly higher than that found in the residue after IMWAE (20 %).

Figure 6 shows the thermograms related to the pyrolysis of clove buds and the solid residues from IMWAE and CH extractions and Table 3, summarizes the experimental temperatures and percentage mass losses of the corresponding degradation steps.

Figure 6

Four different mass losses were identified during the thermal analysis of clove buds and the solid residues from IMWAE and CH extractions. The mass loss below 150 °C is related to the essential oil evaporation in raw clove buds (15.4% at T_{peak}=95 °C) and to moisture evaporation (almost 6% at T_{peak}=50 °C) in solid residues from IMWAE and CH. The mass losses above 150 °C are due to the solid portion of the samples, and they have been assigned in the literature to the pyrolysis of lignocellulosic materials: hemicellulose in the temperature range 215-220 °C, cellulose in the temperature range 315-400 °C and lignin in the temperature range 160-900 °C (Carrier et al., 2011; Sher et al., 2020; Yang et al., 2007).

Table 3

The pyrolytic profiles of the solid residues from IMWAE and CH extractions are identical among them and slightly different to that of raw clove buds. To directly compare the mass losses of lignocellulosic materials of the solid residues from IMWAE and CH extractions to those of raw clove buds the curves have been

rescaled by taking the value at 150 °C as 100%, thus eliminating the mass losses due to essential oil and moisture evaporation. The rescaled mass losses are reported in Table S2 of ESI. The mass losses in the temperature range 150-400 °C highlight a significant decrease (2-3 times) of the hemicellulose/cellulose ratio in both residues respect to raw clove buds, in agreement with PLS data.

Figure 7 shows the profiles of the main gaseous products obtained by monitoring their strongest IR bands (CO2 λ=2371 cm^{-1}, CO λ=2165 cm^{-1}, small-oxygenated compounds λ=1738 cm^{-1} and methane λ=3015 cm^{-1}) evolved during the thermal decomposition of residues after IMWAE (a) and CH (b).

Figure S1 shows the results of TG-FTIR analysis at three significant temperatures (T= 240 °C, 345 °C and 490 °C). The FTIR spectra showed that both IMWAE and CH solid residues evolve similar gases at T=240 °C, i.e. CO_2 (2358, 2322 cm^{-1} O=C=O asymmetric stretching and, 668 cm^{-1} O=C=O bending), CO (2181, 2106 cm^{-1} stretching), H_2O (3736 cm^{-1} OH symmetric stretching) and small oxygenated compounds (aldehydes and carboxylic acids, 1738 cm^{-1} C=O stretching, 2930 cm^{-1} -CH_2- stretching, 2859 cm^{-1} –CH symmetric stretching and methane (3015 cm^{-1} C–H stretching).

It has been reported that CO_2 evolution during lignocellulosic thermal degradation is due to the cracking and reforming of functional groups of carboxyl (C=O) and COOH (Yang et al., 2007). CO_2 is released at all three different temperatures explored (matching with the hemicellulose, cellulose and lignin degradation steps). The intensity of CO_2 signal was higher at lower temperature. The CO_2 production during lignocellulosic material degradation is, indeed, associated to hemicellulose degradation (due to its higher carbonyl content units) (Yang et al., 2007). CO was evolved at higher temperature with two remarkable peaks at 350 and 500 °C (Figure 7). The evolution of CO was mainly related to cellulose decomposition due to the high carbonyl units contained in the cellulose polymer. Lignin decomposition can be observed by following the methane evolution profile. CH_4 evolved mainly after 500 °C due to the thermal cracking of methyl groups contained in lignin (Methoxyl-O-CH_3) (Yang et al., 2007). Thus, the evolution profiles of gases allowed us to identify the three main decomposition steps related to hemicellulose, cellulose and lignin, respectively.

Figure 7

The CO_2 evolution profiles of Figure 7 have different intensity in solid residues obtained after IMWAE and CH. Under the same experimental conditions, the differences in the IR intensity could indicate different

concentration of the gas evolved (Yang et al., 2007). The comparison between the IR intensity of CO_2 signals observed in the evolution profile of solid residues from IMWAE highlighted that the peak with a maximum value at 345 °C (due to the main cellulose decomposition) and the two peaks with lower IR intensity at 240 °C and at 660 °C (due to hemicellulose and lignin decomposition, respectively) correspond to a solid residue with lower amount of hemicellulose and lignin, respectively. A similar behaviour of the IR intensity of CO_2 signals was observed in the evolution profile of solid residues from CH. However, the intensity of all peaks was lower than that observed in the residue from IMWAE (Figure 7(b)). It can be hypothesized that MW irradiation produce a solid residue characterized by the increase of branched hemicellulose hydrolysis and, thus, an enhancement of phenolic compounds extraction (EO and lignin). This effect is expected also during CH but it is more evident in IMWAE due to the acceleration of the extraction process.

A further characterisation of the solid residues from IMWAE and CH, using their corresponding pyrolytic profiles obtained by the non-isothermal thermogravimetric analysis, is in progress through the biomass pyrolysis kinetics investigation.

In the prospective biorefining of clove buds according to Figure 1 the calorimetric combustion of IMWAE and CH residues were determined in order to assess the enthalpy of combustion values ($\Delta_c H$). This information is useful for the alternative uses of solid residues as fuels for energy production.

The standard enthalpy of combustion ($\Delta_c H°$) of the solid residues from IMWAE and CH was calculated using the standard enthalpy of formation ($\Delta_f H°$) reported for hemicellulose, cellulose and lignin components (Gorensek et al., 2019). The biomasses derivate from clove buds showed characteristics of softwoods (Chen et al., 2010), the $\Delta_f H°$ and monomer units for the three components were then selected accordingly: hemicellulose (monomer xylose units, MW = 132.12 g mol^{-1}, $\Delta_f H°$ = –759.2 kJ mol^{-1}), cellulose (monomer glucose unit, MW = 161.14 g mol^{-1}, $\Delta_f H°$ = –1019.0 kJ mol^{-1}) and lignin (monomer unit, MW = 258.27 g mol^{-1}, $\Delta_f H°$ = –759.39 kJ mol^{-1}) (Gorensek et al., 2019). The $\Delta_c H°(i)$ values were calculated by Eq. (2):

$$\Delta_c H^{\circ}(i) = \nu_{CO_2} \Delta_f H^{\circ}_{CO_2} + \nu_{H_2O} \Delta_f H^{\circ}_{H_2O} - \Delta_f H^{\circ}(i) \qquad (2)$$

(i = hemicellulose, cellulose, lignin)

Where $\Delta_f H°CO_2$= -393.51 kJ mol^{-1} and $\Delta_f H°H_2O$= -285.83 kJ mol^{-1} are the standard enthalpies of formation of carbon dioxide and liquid water, respectively and νCO_2 and νH_2O are the stoichiometric coefficients of CO_2 and H_2O in each combustion reaction:

$$Hemicellulose: \quad C_5H_8O_4 + 5O_2 \rightarrow 5CO_2 + 4H_2O$$

$$Cellulose: \quad C_6H_{10}O_5 + 6O_2 \rightarrow 6CO_2 + 5H_2O$$

$$Lignin: \quad C_{15}H_{14}O_4 + 33(\frac{1}{2})O_2 \rightarrow 15CO_2 + 7H_2O$$

The combustion enthalpy values calculated by Eq. (2) for hemicellulose, cellulose and lignin are $\Delta_c H°hemi$= -2351.67 kJ mol^{-1}, $\Delta_c H°cell$= -2771.21 kJ mol^{-1} and $\Delta_c H°lig$= -7144.07 kJ mol^{-1}.

From the known values of the percentage compositions in hemicellulose cellulose, and lignin, assumed as to be the only burning components, the combustion enthalpy of the biomass can then be calculated:

$$\Delta_c H_{biomass}/kJ\ g^{-1} = \frac{\sum_{i=1}^{3}(\%_i \frac{\Delta_c H_i^{\circ}/kJmol^{-1}}{MW_i/gmol^{-1}})}{100} \qquad (3)$$

(i = hemicellulose, cellulose, lignin)

Table 4 shows the $\Delta_c H$ for solid residues from IMWAE and CH calculated from the percentage composition of Table 2 (obtained by FTIR chemometrics) according to Eq. (3) compared with experimental values obtained by direct calorimetry and with the higher heating value reported for solid residues from clove buds treated with a MW process (Kapadiya et al., 2018). Two different values were calculated for each sample from the percentages of FTIR PLS analysis data.

The first value is calculated considering only the lignin content found with the chemometric method as is, therefore, is expected to be underestimated. The second value considers the total lignin, that is also the degraded fraction missed by PLS analysis, by attributing to it the same heat of combustion as lignin. The latter value is therefore expected to be overestimated.

Thus, the enthalpy of combustion of the solid residue from IMWAE should be between –15.40 and –18.41 kJ g^{-1} and that from CH should be between –16.60 and –19.00 kJ g^{-1}. This is consistent with the experimental values.

560 **Table 4**

561

562 The experimental $-\Delta_c H$ (kJ g^{-1}) values of solid residues from IMWAE and CH (Table 4) are in line with
563 those reported for lignocellulose woods (i.e. pine ($-\Delta_c H$=20.68 kJ g^{-1}), spruce ($-\Delta_c H$=20.5 kJ g^{-1}), poplar
564 ($-\Delta_c H$=19.57 kJ g^{-1}), bagasse ($-\Delta_c H$=18.82 kJ g^{-1}), corn stalks ($-\Delta_c H$=18.60 kJ g^{-1}), sweetgrass (–
565 $\Delta_c H$=18.66 kJ g^{-1}), wheat straw($-\Delta_c H$=18.43 kJ g^{-1})) (Ioelovich, 2018). The calculated $-\Delta_c H$ (kJ g^{-1}) using
566 the composition predicted by PLS of FTIR spectra are in a reasonable agreement with the experimental
567 values and the HHV reported. The $\Delta_c H$ highlights the energetic features of solid residues from IMWAE
568 and CH for their potential uses as alternative biomass for fuel production.

569 **Conclusions**

570

571 Full valorization of aromatic herbs through an energy efficient and eco-friendly approaches addresses well
572 the goals of the agenda 2030 for sustainable development of the United Nations (Marco et al., 2020).

573 The chemical characterization of the three products obtained after IMWAE of clove buds and the
574 quantification of their main components (EOs, polyphenols in the condensed water and solid residue)
575 proposed in this work represents an essential step for their further valorization and exploitation. Moreover,
576 the IMWAE here proposed represents a green, competitive and economically attractive approach easily
577 applicable to a wide gamma of different substrates like aromatic herbs, spices and seeds and it may suggest
578 how to increase the shareholder value, and to maximize the profit of these novel hydrodistillation processes
579 (Gonzalez Rivera et al., 2016; Santana-Méridas et al., 2014), in agreement with the concept of biorefinery
580 and sustainable chemistry (Corona et al., 2018; Gonzalez-Rivera et al., 2016; Rombaut et al., 2014).

581 IMWAE has the following technological advantages: i) the use of several independent coaxial antennas
582 applied in situ should permit to extend MW irradiation to very large batch reactors (pilot plants) as well as
583 to continuous flow systems (production scale); (ii) any problem due to high processable volumes is in
584 principle overcome because the method offers the possibility of breaking the scale-up and scale-out barrier
585 in industrial processes, enabling a better control of the local temperature and of its distribution, in
586 comparison with other microwave systems commonly employed; (iii) due to its versatility, this method can
587 be applied to most of the process technologies already available; (iv) the proposed microwave extractor is

588 not a resonant cavity applicator, so that it is apart from the conventional definition and differentiation
589 between multi-mode and mono-mode conventional microwave instruments.

590 Unimportantly, the biorefining of clove bud components, well known for their antiviral effect can open new
591 opportunities for the exploitation and application of low cost, worldwide available and naturally-occurring
592 antivirals to the treatment of current and future outbreak pandemic emergences.

593

594 Credit authorship contribution statement

595 José Gonzalez-Rivera, Celia Duce, Beatrice Campanella, Carlo Ferrari, Iginio Longo, Luca Bernazzani,
596 Emilia Bramanti: Conceptualization, Methodology, Investigation. José Gonzalez-Rivera, Celia Duce, Luca
597 Bernazzani, Emilia Bramanti: writing - original draft. José Gonzalez-Rivera, Celia Duce, Beatrice
598 Campanella, Eleonora Tanzini, Massimo Onor, Luca Bernazzani, Julian Cabrera Ruiz: Data curation.
599 Writing, review & editing and supervision, funding acquisition: Maria Rosaria Tinè, Celia Duce, Carlo
600 Ferrari, Beatrice Campanella, Luca Bernazzani, Maria Rosaria Tinè, Emilia Bramanti.

601 Declaration of Competing Interest

602 The authors declare that they have no known competing financial interests or personal relationships that
603 could have appeared to influence the work reported in this paper.

604 Acknowledgments

605 The authors would like to thank C. Lanza and A. Barbini (INO-CNR), M. Cempini (ICCOM-CNR), E.
606 Pulidori and R. Carosi (Dipartimento di Chimica e Chimica Industriale, Università di Pisa) for their
607 valuable technical support.

608 References

609

610 Adefegha, S.A., Oboh, G., Oyeleye, S.I., Osunmo, K., 2016. Alteration of starch hydrolyzing enzyme
611 inhibitory properties, antioxidant activities, and phenolic profile of clove buds (Syzygium
612 aromaticum L.) by cooking duration. Food Sci. Nutr. 4, 250–260. https://doi.org/10.1002/fsn3.284

Al-taee, H., Azimullah, S., Meeran, M.F.N., Almheiri, K.M.A., Jasmi, A.R. Al, Tariq, S., Khan, M.A., Adeghate, E., Ojha, S., 2019. β-caryophyllene, a dietary phytocannabinoid attenuates oxidative stress, inflammation, apoptosis and prevents structural alterations of the myocardium against doxorubicin-induced acute cardiotoxicity in rats: An in vitro and in vivo study. Eur. J. Pharmacol. 858, 172467. https://doi.org/10.1016/j.ejphar.2019.172467

Alexandru, L., Cravotto, G., Giordana, L., Binello, A., Chemat, F., 2013. Ultrasound-assisted extraction of clove buds using batch- and flow-reactors: A comparative study on a pilot scale. Innov. Food Sci. Emerg. Technol. 20, 167–172. https://doi.org/10.1016/j.ifset.2013.07.011

Ascrizzi, R., González-Rivera, J., Pomelli, C.S., Chiappe, C., Margari, P., Costagli, F., Longo, I., Tiné, M.R., Flamini, G., Duce, C., 2017. Ionic liquids, ultra-sounds and microwaves: An effective combination for a sustainable extraction with higher yields. the cumin essential oil case. React. Chem. Eng. 2, 577–589. https://doi.org/10.1039/c7re00075h

Assefa, A.D., Keum, S.Y., Saini, K.R., 2018. A comprehensive study of polyphenols contents and antioxidant potential of 39 widely used spices and food condiments. J. Food Meas. Charact. 12, 1548–1555. https://doi.org/10.1007/s11694-018-9770-z

Bagherian, H., Zokaee Ashtiani, F., Fouladitajar, A., Mohtashamy, M., 2011. Comparisons between conventional, microwave- and ultrasound-assisted methods for extraction of pectin from grapefruit. Chem. Eng. Process. Process Intensif. 50, 1237–1243. https://doi.org/10.1016/j.cep.2011.08.002

Bramanti, E., Fulgentini, L., Bizzarri, R., Lenci, F., Sgarbossa, A., 2013. Beta-amyloid amorphous aggregates induced by the small natural molecule ferulic acid. J. Phys. Chem. B 117. https://doi.org/10.1021/jp4079986

Bramanti, E., Lenci, F., Sgarbossa, A., 2010. Effects of hypericin on the structure and aggregation properties of beta-amyloid peptides. Eur. Biophys. J. 39. https://doi.org/10.1007/s00249-010-0607-x

Calinescu, I., Lavric, V., Asofiei, I., Gavrila, A.I., Trifan, A., Ighigeanu, D., Martin, D., Matei, C., 2017. Microwave assisted extraction of polyphenols using a coaxial antenna and a cooling system. Chem. Eng. Process. Process Intensif. 122, 373–379. https://doi.org/https://doi.org/10.1016/j.cep.2017.02.003

Carrier, M., Loppinet-serani, A., Denux, D., Lasnier, J., Ham-Pichavant, F., Cansell, F., Aymonier, C., 2011. Thermogravimetric analysis as a new method to determine the lignocellulosic composition of biomass. Biomass and Bioenergy 35, 298–307. https://doi.org/10.1016/j.biombioe.2010.08.067

Cassiana Frohlich, P., Andressa Santos, K., Palú, F., Cardozo-filho, L., da Silva, C., da Silva, E.A., 2019. Evaluation of the effects of temperature and pressure on the extraction of eugenol from clove (Syzygium aromaticum) leaves using supercritical CO2. J. Supercrit. Fluids 143, 313–320.

https://doi.org/10.1016/j.supflu.2018.09.009
Catel-Ferreira, M., Tnani, H., Hellio, C., Cosette, P., Lebrun, L., 2015. Antiviral effects of polyphenols: Development of bio-based cleaning wipes and filters. J. Virol. Methods 212, 1–7. https://doi.org/10.1016/j.jviromet.2014.10.008
Chen, H., Ferrari, C., Angiuli, M., Yao, J., Raspi, C., Bramanti, E., 2010. Qualitative and quantitative analysis of wood samples by Fourier transform infrared spectroscopy and multivariate analysis. Carbohydr. Polym. 82, 772–778. https://doi.org/10.1016/j.carbpol.2010.05.052
Chiow, K.H., Phoon, M.C., Putti, T., Tan, B.K.H., Chow, V.T., 2016. Evaluation of antiviral activities of Houttuynia cordata Thunb. extract, quercetin, quercetrin and cinanserin on murine coronavirus and dengue virus infection. Asian Pac. J. Trop. Med. 9, 1–7. https://doi.org/https://doi.org/10.1016/j.apjtm.2015.12.002
Clifford, A.A., Basile, A., Al-saidi, S.H.R., 1999. A comparison of the extraction of clove buds with supercritical carbon dioxide and superheated water. Fresenius J Anal Chem 364, 635–637.
Corona, A., Parajuli, R., Ambye-Jensen, M., Hauschild, M., Birkved, M., 2018. Environmental screening of potential biomass for green biorefinery conversion. J. Clean. Prod. 189, 344–357. https://doi.org/10.1016/J.JCLEPRO.2018.03.316
Cortés-Rojas, D.F., de Souza, C.R.F., Oliveira, W.P., 2014. Clove (Syzygium aromaticum): a precious spice. Asian Pac. J. Trop. Biomed. 4, 90–96. https://doi.org/https://doi.org/10.1016/S2221-1691(14)60215-X
Dai, J.-P., Zhao, X.-F., Zeng, J., Wan, Q.-Y., Yang, J.-C., Li, W.-Z., Chen, X.-X., Wang, G.-F., Li, K.-S., 2013. Drug screening for autophagy inhibitors based on the dissociation of Beclin1-Bcl2 complex using BiFC technique and mechanism of eugenol on anti-influenza A virus activity. PLoS One 8, e61026. https://doi.org/10.1371/journal.pone.0061026
de Oliveira, A., Prince, D., Lo, C.-Y., Lee, L.H., Chu, T.-C., 2015. Antiviral activity of theaflavin digallate against herpes simplex virus type 1. Antiviral Res. 118, 56–67. https://doi.org/10.1016/j.antiviral.2015.03.009
Deng, J., Yang, B., Chen, C., Liang, J., 2015. Renewable Eugenol-Based Polymeric Oil-Absorbent Microspheres: Preparation and Oil Absorption Ability. ACS Sustain. Chem. Eng. 3, 599–605. https://doi.org/10.1021/sc500724e
Derosa, G., Maffioli, P., D'Angelo, A., Di Pierro, F., 2020. A role for quercetin in coronavirus disease 2019 (COVID-19). Phyther. Res. n/a. https://doi.org/10.1002/ptr.6887
Dua, A., Singh, A., Mahajan, R., 2015. Antioxidants of clove (Syzygium aromaticum) prevent metal induced oxidative damage of biomolecules. Int. Res. J. Pharm. 6, 273–278.

https://doi.org/10.7897/2230-8407.06460
Fidyt, K., Fiedorowicz, A., Strzadala, L., Szumny, A., 2016. β-caryophyllene and β-caryophyllene oxide-natural compounds of anticancer and analgesic properties. Cancer Med. 5, 3007–3017. https://doi.org/10.1002/cam4.816
Golmakani, M., Rezaei, K., 2008. Comparison of microwave-assisted hydrodistillation with the traditional hydrodistillation method in the extraction of essential oils from Thymus vulgaris L . 109, 925–930. https://doi.org/10.1016/j.foodchem.2007.12.084
Golmakani, M., Zare, M., Razzagi, S., 2017. Eugenol enrichment of clove bud essential oil using different microwave-assisted distillation methods. Food Sci. Technol. Res. 23, 385–394. https://doi.org/10.3136/fstr.23.385
González-Rivera, J., Galindo-Esquivel, I.R., Onor, M., Bramanti, E., Longo, I., Ferrari, C., 2014. Heterogeneous catalytic reaction of microcrystalline cellulose in hydrothermal microwave-assisted decomposition: effect of modified zeolite Beta. Green Chem. 16, 1417. https://doi.org/10.1039/c3gc42207k
Gonzalez-Rivera, J., Spepi, A., Ferrari, C., Duce, C., Longo, I., Falconieri, D., Piras, A., Tiné, M.R., 2016. Novel configurations for a citrus waste based biorefinery: from solventless to simultaneous ultrasound and microwave assisted green extraction. Green Chem. 18, 6482–6492.
Gonzalez Rivera, J., Duce, C., Falconieri, D., Ferrari, C., Ghezzi, L., Piras, A., Tine´, M.R., 2016. Coaxial Microwave assisted hydrodistillation of essential oils from five different herbs (lavender , rosemary , sage , fennel seeds and clove buds): chemical composition and thermal analysis Authors : J. Innov. Food Sci. Emerg. Technol. 33, 308–318.
Gorensek, M.B., Shukre, R., Chen, C.C., 2019. Development of a thermophysical properties model for flowsheet simulation of biomass pyrolysis processes. ACS Sustain. Chem. Eng. 7, 9017–9027. https://doi.org/10.1021/acssuschemeng.9b01278
Grumezescu, A.M., Vasile, B. Ș, Holban, A.M., 2013. Eugenol functionalized magnetite nanostructures used in anti-infectious therapy. Lett. Appl. nanobioscience 2, 120–123.
Guan, W., Li, S., Yan, R., Tang, S., Quan, C., 2007. Comparison of essential oils of clove buds extracted with supercritical carbon dioxide and other three traditional extraction methods. Food Chem. 101, 1558–1564. https://doi.org/10.1016/j.foodchem.2006.04.009
Hadidi, M., Pouramin, S., Adinepour, F., Haghani, S., Jafari, S.M., 2020. Chitosan nanoparticles loaded with clove essential oil: characterization, antioxidant and antibacterial activities. Carbohydr. Polym. 236, 116075. https://doi.org/https://doi.org/10.1016/j.carbpol.2020.116075
Hume, W.R., 1986. The pharmacologic and toxicological properties of zinc oxide-eugenol. J. Am. Dent.

712 Assoc. 113, 789–791. https://doi.org/10.14219/jada.archive.1986.0256
713 Ioelovich, M., 2018. Thermodynamics of biomass-based solid fuels. Acad. J. Polym. Sci. 2.
714 https://doi.org/10.19080/ajop.2018.02.555577
715 Jassim, S.A.A., Naji, M.A., 2003. Novel antiviral agents: a medicinal plant perspective. J. Appl.
716 Microbiol. 95, 412–427. https://doi.org/10.1046/j.1365-2672.2003.02026.x
717 Jiao, Y., Wan, C., Li, J., 2017. Scalable synthesis and characterization of free-standing supercapacitor
718 electrode using natural wood as a green substrate to support rod-shaped polyaniline. J. Mater. Sci.
719 Mater. Electron. 28, 2634–2641. https://doi.org/10.1007/s10854-016-5840-3
720 Kang, S., Li, X., Fan, J., Chang, J., 2013. Hydrothermal conversion of lignin: A review. Renew. Sustain.
721 Energy Rev. 27, 546–558. https://doi.org/https://doi.org/10.1016/j.rser.2013.07.013
722 Kapadiya, S.M., Parikh, J., Desai, M.A., 2018. A greener approach towards isolating clove oil from buds
723 of Syzygium aromaticum using microwave radiation. Ind. Crop. Prod. 112, 626–632.
724 https://doi.org/10.1016/j.indcrop.2017.12.060
725 Kazuo, N., Yoshikatzu, T., 1997. Gargling cup, antiviral mask, antiviral filter, antifungal, antibacterial,
726 and antiviral filter air cleaner and air-cleaner humidifier.
727 Khalil, A.A., Rahman, U. u, Khan, M.R., Sahar, A., Mehmood, T., Khan, M., 2017. Essential oil eugenol:
728 sources, extraction techniques and nutraceutical perspectives. RSC Adv. 7, 32669–32681.
729 https://doi.org/10.1039/c7ra04803c
730 Khan, A., Qadir, S.S., Khattak, K.N., Anderson, R.A., 2006. Cloves improve glucose, cholesterol and
731 triglycerides of people with type 2 diabetes mellitus. FASEB J. 20, A990–A990.
732 Lane, T., Anantpadma, M., Freundlich, J.S., Davey, R.A., Madrid, P.B., Ekins, S., 2019. The natural
733 product eugenol is an inhibitor of the Ebola virus in vitro. Pharm. Res. 36, 104.
734 https://doi.org/10.1007/s11095-019-2629-0
735 Lee, K.G., Shibamoto, T., 2001. Antioxidant property of aroma extract isolated from clove buds
736 [Syzygium aromaticum (L.) Merr. et Perry]. Food Chem. 74, 443–448.
737 https://doi.org/10.1016/S0308-8146(01)00161-3
738 Leon-méndez, G., Osorio-fortich, M., Ortega-toro, R., Pajaro-castro, N., Torrenegra-alarcón, M., Herrera-
739 barros, A., 2018. Design of an emulgel-type cosmetic with antioxidant activity asing active essential
740 oil microcapsules of thyme (Thymus vulgaris L.), cinnamon (Cinnamomum verum J.), and clove
741 (Eugenia caryophyllata T.). Int. J. Polym. Sci. 2018, 1–16.
742 Longo, I., Ricci, A.S., 2007. Chemical activation using an open-end coaxial applicator. J. Microw. Power
743 Electromagn. Energy 41, 4–19.
744 Marchese, A., Barbieri, R., Coppo, E., Orhan, I.E., Daglia, M., Nabavi, S.F., Izadi, M., Abdollahi, M.,

745 Nabavi, S.M., Ajami, M., 2017. Antimicrobial activity of eugenol and essential oils containing
746 eugenol: A mechanistic viewpoint. Crit. Rev. Microbiol. 43, 668–689.
747 https://doi.org/10.1080/1040841X.2017.1295225
748 Marco, M. Di, Baker, M.L., Daszak, P., de Barro, P., Eskew, E.A., Godde, C.M., Harwood, T.D.,
749 Herrero, M., Hoskins, A.J., Johnson, E., Karesh, W.B., Machalaba, C., Garcia, J.N., Paini, D., Pirzl,
750 R., Smith, M.S., Zambrana-Torrelio, C., Ferrier, S., 2020. Sustainable development must account for
751 pandemic risk. Proc. Natl. Acad. Sci. U. S. A. 117, 3888–3892.
752 https://doi.org/10.1073/pnas.2001655117
753 Mukhtar, M., Arshad, M., Ahmad, M., Pomerantz, R.J., Wigdahl, B., Parveen, Z., 2008. Antiviral
754 potentials of medicinal plants. Virus Res. 131, 111–120.
755 https://doi.org/https://doi.org/10.1016/j.virusres.2007.09.008
756 Munoz Castellanos, L., Amaya Olivas, N., Ayala-Soto, J., Contreras, C.M.D.L.O., Zermeno Ortega, M.,
757 Sandoval Salas, F., Hernandez-Ochoa, L., 2020. In vitro and in vivo antifungal activity of clove
758 (Eugenia caryophyllata) and pepper (Piper nigrum L.) essential oils and functional extracts against
759 Fusarium oxysporum and Aspergillus niger in tomato (Solanum lycopersicum L.). Int. J. Microbiol.
760 2020. https://doi.org/10.1155/2020/1702037
761 Nirmala, M.J., Durai, L., Gopakumar, V., Nagarajan, R., 2019. Anticancer and antibacterial effects of a
762 clove bud essential oil-based nanoscale emulsion system. Int. J. Nanomedicine 14, 6439–6450.
763 https://doi.org/10.2147/IJN.S211047
764 Omar, S.H., 2010. Oleuropein in olive and its pharmacological effects. Sci. Pharm. 78, 133–154.
765 https://doi.org/10.3797/scipharm.0912-18
766 Pandey, K.B., Rizvi, S.I., 2009. Plant polyphenols as dietary antioxidants in human health and disease.
767 Oxid. Med. Cell. Longev. 2, 270–278.
768 Petigny, L., Périno, S., Minuti, M., Visinoni, F., Wajsman, J., Chemat, F., 2014. Simultaneous microwave
769 extraction and separation of volatile and non-volatile organic compounds of boldo leaves. From lab
770 to industrial scale. Int. J. Mol. Sci. 15, 7183–98. https://doi.org/10.3390/ijms15057183
771 Pingret, D., Fabiano-Tixier, A.S., Chemat, F., 2014. An improved ultrasound clevenger for extraction of
772 essential oils. Food Anal. Methods 7, 9–12. https://doi.org/10.1007/s12161-013-9581-0
773 Rassem, H.H.A., Nour, A.H., Yunus, R.M., 2016. Techniques for extraction of essential oils from plants :
774 a review. Aust. J. Basic Appl. Sci. 10, 117–127.
775 Reverchon, E., Marrone, C., 1997. Supercritical extraction of clove bud essential oil : isolation and
776 mathematical modeling. Chem. Eng. Sci. 52, 3421–3428.
777 Roldán-Gutiérrez, J.M., Ruiz-Jiménez, J., Luque de Castro, M.D., 2008. Ultrasound-assisted dynamic

778 extraction of valuable compounds from aromatic plants and flowers as compared with steam
779 distillation and superheated liquid extraction. Talanta 75, 1369–75.
780 https://doi.org/10.1016/j.talanta.2008.01.057
781 Rombaut, N., Tixier, A.-S., Bily, A., Chemat, F., 2014. Green extraction processes of natural products as
782 tools for biorefinery. Biofuels, Bioprod. Biorefining 8, 530–544.
783 Saleh, I.A., Vinatoru, M., Mason, T.J., Abdel-Azim, N.S., Aboutabl, E.A., Hammouda, F.M., 2016. A
784 possible general mechanism for ultrasound-assisted extraction (UAE) suggested from the results of
785 UAE of chlorogenic acid from Cynara scolymus L. (artichoke) leaves. Ultrason. Sonochem. 31,
786 330–336. https://doi.org/10.1016/j.ultsonch.2016.01.002
787 Santana-Méridas, O., Polissiou, M., Izquierdo-Melero, M.E., Astraka, K., Tarantilis, P.A., Herraiz-
788 Peñalver, D., Sánchez-Vioque, R., 2014. Polyphenol composition, antioxidant and bioplaguicide
789 activities of the solid residue from hydrodistillation of Rosmarinus officinalis L. Ind. Crops Prod. 59,
790 125–134. https://doi.org/10.1016/j.indcrop.2014.05.008
791 Schimdt, E., 2010. Handbook of Essential Oils Science, Technology, and applications, I. ed. Taylor and
792 Francis Group, LLC, Boca Raton, FL.
793 Scopel, R., Falcão, M.A., Lucas, A.M., Almeida, R.N., Gandolfi, P.H.K., Cassel, E., Vargas, R.M.F.,
794 2014. Supercritical fluid extraction from Syzygium aromaticum buds: Phase equilibrium ,
795 mathematical modeling and antimicrobial activity. J. Supercrit. Fluids 92, 223–230.
796 https://doi.org/10.1016/j.supflu.2014.06.003
797 Sgarbossa, A., Monti, S., Lenci, F., Bramanti, E., Bizzarri, R., Barone, V., 2013. The effects of ferulic
798 acid on beta-amyloid fibrillar structures investigated through experimental and computational
799 techniques. Biochim. Biophys. Acta - Gen. Subj. 1830. https://doi.org/10.1016/j.bbagen.2012.12.023
800 Sher, F., Iqbal, S.Z., Liu, H., Imran, M., Snape, C.E., 2020. Thermal and kinetic analysis of diverse
801 biomass fuels under different reaction environment : A way forward to renewable energy sources.
802 Energy Convers. Manag. 203, 112266. https://doi.org/10.1016/j.enconman.2019.112266
803 Sivanesam, K., Andersen, N., 2019. Pre-structured hydrophobic peptide β-strands: A universal amyloid
804 trap? Arch. Biochem. Biophys. 664, 51–61. https://doi.org/https://doi.org/10.1016/j.abb.2019.01.032
805 Song, J.-M., Lee, K.-H., Seong, B.-L., 2005. Antiviral effect of catechins in green tea on influenza virus.
806 Antiviral Res. 68, 66–74. https://doi.org/https://doi.org/10.1016/j.antiviral.2005.06.010
807 Tekin, K., Akalin, M.K., Seker, M.G., 2015. Ultrasound bath-assisted extraction of essential oils from
808 clove using central composite design. Ind. Crop. Prod. 77, 954–960.
809 https://doi.org/10.1016/j.indcrop.2015.09.071
810 Tiwari, B.K., 2015. Ultrasound: A clean, green extraction technology. TrAC - Trends Anal. Chem. 71,

100–109. https://doi.org/10.1016/j.trac.2015.04.013
Toledano, A., Serrano, L., Pineda, A., Romero, A.A., Luque, R., Labidi, J., 2014. Microwave-assisted depolymerisation of organosolv lignin via mild hydrogen-free hydrogenolysis: Catalyst screening. Appl. Catal. B Environ. 145, 43–55. https://doi.org/https://doi.org/10.1016/j.apcatb.2012.10.015
TOXNET. Toxycologycal data network: Eugenol [WWW Document], n.d.
Uddin, M.A., Shahinuzzaman, M., Rana, M.S., Yaakob, Z., 2017. Stusy of chemical composition and medicinal properties of volatile oil from clove buds (Eugenia Caryophyllus). Int. J. Pharm. Sci. Res. 8, 895–899. https://doi.org/10.13040/IJPSR.0975-8232.8(2).895-99
Uju, D.E., Obioma, N.P., 2011. Anticariogenic potentials of clove , tobacco and bitter kola. Asian Pac. J. Trop. Med. 4, 814–818. https://doi.org/10.1016/S1995-7645(11)60200-9
Wan, J., Jin, Z., Zhong, S., Schwarz, P., Chen, B., Rao, J., 2020. Clove oil-in-water nanoemulsion: Mitigates growth of Fusarium graminearum and trichothecene mycotoxin production during the malting of Fusarium infected barley. FOOD Chem. 312. https://doi.org/10.1016/j.foodchem.2019.126120
Yamada, K., Ogawa, H., Hara, A., Yoshida, Y., Yonezawa, Y., Karibe, K., Nghia, V.B., Yoshimura, H., Yamamoto, Y., Yamada, M., Nakamura, K., Imai, K., 2009. Mechanism of the antiviral effect of hydroxytyrosol on influenza virus appears to involve morphological change of the virus. Antiviral Res. 83, 35–44. https://doi.org/https://doi.org/10.1016/j.antiviral.2009.03.002
Yang, H., Yan, R., Chen, H., Ho-Lee, D., Zheng, C., 2007. Characteristics of hemicellulose , cellulose and lignin pyrolysis. Fuel 86, 1781–1788. https://doi.org/10.1016/j.fuel.2006.12.013
Yang, Y., Wei, M., Hong, S., 2014. Ultrasound-assisted extraction and quantitation of oils from Syzygium aromaticum flower bud (clove) with supercritical carbon dioxide. J. Chromatogr. A 1323, 18–27. https://doi.org/10.1016/j.chroma.2013.10.098
Zhang, D., Wu, K., Zhang, X., Deng, S., Peng, B., 2020. In silico screening of Chinese herbal medicines with the potential to directly inhibit 2019 novel coronavirus. J. Integr. Med. 18, 152–158. https://doi.org/https://doi.org/10.1016/j.joim.2020.02.005
Zhong, Y., Ma, C.-M., Shahidi, F., 2012. Antioxidant and antiviral activities of lipophilic epigallocatechin gallate (EGCG) derivatives. J. Funct. Foods 4, 87–93. https://doi.org/https://doi.org/10.1016/j.jff.2011.08.003
Zuin, V.G., Segatto, M.L., Ramin, L.Z., 2018. Plants as resources for organic molecules: facing the green and sustainable future today. Curr. Opin. Green Sustain. Chem. 9, 1–7. https://doi.org/10.1016/j.cogsc.2017.10.001

TABLES

Table 1. Literature reports of clove buds extracts isolated by different approaches and comparison with the IMWAE developed in this work.

Approach	Source	Extraction conditions			Characterization of extracts				Ref.
					EO		Hydrosoluble Polyphenols (mg/g)	Solid residue analysis	
		Time, min	S/L ratio (w/w)	Solvent	Yield % (wt)	Main compounds (%)			
IMWAE	Indonesia	90	1:40	H_2O	16	eugenol (48.9) β-caryophyllene (42.8) α -caryophyllene (3.7)	Gallic acid (10.4) Chlorogenic acid (1.9) Eugenol (10.4)	*FTIR (PLS model)* Hemicellulose 20±1 % Cellulose 40±4% Lignin 30±3% $-\Delta_cH$= 17.07[a]	This work
CH		120			7.8	eugenol (49.2) β-caryophyllene (43.5) α-caryophyllene (3.8)	Gallic acid (13.9) Chlorogenic acid (1.7) Eugenol (33.5)	*FTIR (PLS model)* Hemicellulose 24±1% Cellulose 31±3% Lignin 34±4% $-\Delta_cH$=17.62[a]	
IMWAE	Madagascar	120	1:5	H_2O	5.9	eugenol (66.9) β-caryophyllene (24.8) α-humulene (3.1)	no	no	(Gonzalez Rivera et al., 2016)
CH		360			9.7	eugenol (87.1) eugenyl acetate (6.4) β-caryophyllene (5.1)			
SD		240	1:20	Steam	18.2	eugenol (81.1) eugenyl acetate (18.1) α –caryophyllene (0.7)			
Soxhlet		1440	----	CH_2Cl_2	17.4	eugenol (76.8) eugenyl acetate (15.2) β-caryophyllene (7.9)			
SHWE	Madagascar	100	----	Superheated water (150°C)	18.3	eugenol (83.6) eugenyl acetate (16.1) β-caryophyllene (1.0)	no	no	(Clifford et al., 1999)
SFE		200 bar-55 °C-330 min		SC-CO_2	21.5	eugenol (76.2) eugenyl acetate (15.7) β-caryophyllene (8.1)			
MAE	India[b]	30	1:6.7	H_2O	13.1	eugenol (90.1)	TPC of hydrosol (83.58 mg GAE/g)	Proposed as alternative source of fuel(i.e. coal)	(Kapadiya et al., 2018)
CH		180	1:25		12.5	eugenol (88.1)			

MAE		80		H_2O	13.9	eugenol (88.8) eugenyl acetate (7.5) β-caryophyllene (2.7)			
MASE	Iran[b]	80	1:10	steam	12.7	eugenol (83.4) eugenyl acetate (14.3) β-caryophyllene (1.4)	no	no	(Golmakani et al., 2017)
CH		240		H_2O	13.0	eugenol (87.3) eugenyl acetate (10.4) β-caryophyllene (1.4)			
SD		240		steam	11.5	eugenol (82.7) eugenyl acetate (15.6) β-caryophyllene (0.9)			
MWHD		40	1:1	H_2O	3.2	eugenol (65.2) β-caryophyllene (12.1)	no	no	(Leon-méndez et al., 2018)
CH		180			2.9	eugenol (60.3) β-caryophyllene (11.6)			
SFE		90 bar-50°C		SC-CO_2	20.8	eugenol (65.9) eugenyl acetate (19.0) β-caryophyllene (11.1)	no	no	(Reverchon and Marrone, 1997)
SFE		100 bar-50°C-120 min		SC-CO_2	19.6	eugenol (58.8) eugenyl acetate (19.6) β-caryophyllene (14.0)			
SD	China[b]	600	1:5	steam	10.1	eugenol (58.2) β-caryophyllene (20.6) eugenyl acetate (13.8)	no	no	(Guan et al., 2007)
CH		360		H_2O	11.5	eugenol (48.8) β-caryophyllene (36.9) α-humulene (4.4)			
Soxhlet		360	1:8.3	Ethanol	41.8	eugenol (57.2) eugenyl acetate (19.4) β-caryophyllene (17.5)			
SFE		90 bar-40°C-240 min		SC-CO_2	14.2	eugenol (63.5) eugenyl acetate (18.8) β-caryophyllene (13.7)	no	no	(Scopel et al., 2014)
US-SFE	Taiwan[b]	150 bar-40°C-115 min		SC-CO_2	22.1	eugenol (59.2) eugenyl acetate (18.6) β-caryophyllene (15.4)	no	no	(Yang et al., 2014)

SFE		200 bar-40°C-170 min			19.1	eugenol (55.6) eugenyl acetate (17.1) β-caryophyllene (14.5)			
SE		360	1:20	Hexane	17.5	eugenol (34.1) eugenyl acetate (10.5) β-caryophyllene (9.1)			
UAE	India	45	1:20	Ethanol : H2O (1:1)	41	α-humulene (≈32) eugenol (≈8) eugenyl acetate (≈5)	TPC of crude extracts (191 ± 1 to 215 ± 3 mg GAE/L)	no	(Alexandru et al., 2013)
	China				41	α-humulene (≈45) eugenol (≈9) eugenyl acetate (≈8)			
	Madagascar				39	α-humulene (≈26) eugenol (≈9) β-caryophyllene(≈5)			
UAE	Turkey[b]	45	1:20	Ethanol	28.2	eugenol (64) α-caryophyllene (n.r.)	no	no	(Tekin et al., 2015)

MWHD=microwave assisted hydrodistillation; CH=hydrodistillation; MAE=microwave assisted extraction; SFE=Supercritical fluid extraction; MASD=microwave-assisted steam distillation; US-SFE=ultrasound-assisted supercritical fluid extraction, UAE=ultrasound assisted extraction; SD=steam distillation; SE=solvent extraction; SHWE=superheated water extraction. S/L=solid/liquid. [a] Experimental enthalpy of combustion (kJ/g); [b] clove buds purchased from local market in the country stated; the native production of the plant is not mentioned.

Table 2. PLS predicted chemical composition of cellulose, hemicellulose and lignin in dry solid residue after the IMWAE and CH (N= 3 replicates).

components	PLS %		
	Raw clove buds	Solid residues after extraction	
		IMWAE	CH
Hemicellulose	25±5	20±1	24±1
Cellulose	19±2	40±4	31±3
Lignin	37±6	18±3	25±4
Insoluble "degraded" lignin[a]	-	12	10
Total lignin	37±6	30±3	35±4
Moisture and volatiles[b]	15±2	6±2	6±2
Ash[c]	5 ±2	2±2	2±2

IMWAE= In situ microwave assisted extraction; CH=hydrodistillation. [a] Calculated by difference; [b] step (I) Table 3 TGA under nitrogen flow; [c] TGA under air flow.

867

868 **Table 3**. Experimental temperatures and percentage mass losses of the corresponding degradation steps
869 under nitrogen flow of raw clove buds and solid residues from IMWAE and CH extractions.
870

Step	Mass loss/wt % (T_{peak}/°C)		
	Raw clove buds	Solid residues after extraction	
		IMWAE	CH
I Volatiles (<150 °C)	15.4 (95)	5.9 (53)	6.1 (52)
II Main degradation of hemicellulose and cellulose (150-400 °C)	15.0 (220) 27.9 (327)	10.5 (235) 40.6 (340)	11.0 (236) 39.3 (338)
III Main degradation of lignin (400-800 °C)	17.1 (405, 460, 632)	19.9 (407, 485, 632)	20.3 (407, 485, 632)
Residual mass at 900 °C	24.6	23.1	23.3

871 IMWAE= In situ microwave assisted extraction; CH=hydrodistillation.

872

873

874

875

Table 4. $\Delta_c H$ for solid residues from IMWAE and CH.

	$-\Delta_c H$ (kJ/g)		
Estimation method	solid residue from IMWAE	solid residue from CH	Reference
FTIR chemometrics	15.40[a] 18.41[b]	16.60[a] 19.00[b]	This work
Experimental Combustion calorimetry	17.07	17.62	This work
Higher heating value	21.1758	---	(Kapadiya et al., 2018)

IMWAE= In situ microwave assisted extraction; CH=hydrodistillation; $\Delta_c H$= enthalpy of combustion. [a] Calculated considering only the lignin content found with the chemometric method; [b] Calculate accounting also for "degraded" lignin (see text).

FIGURES

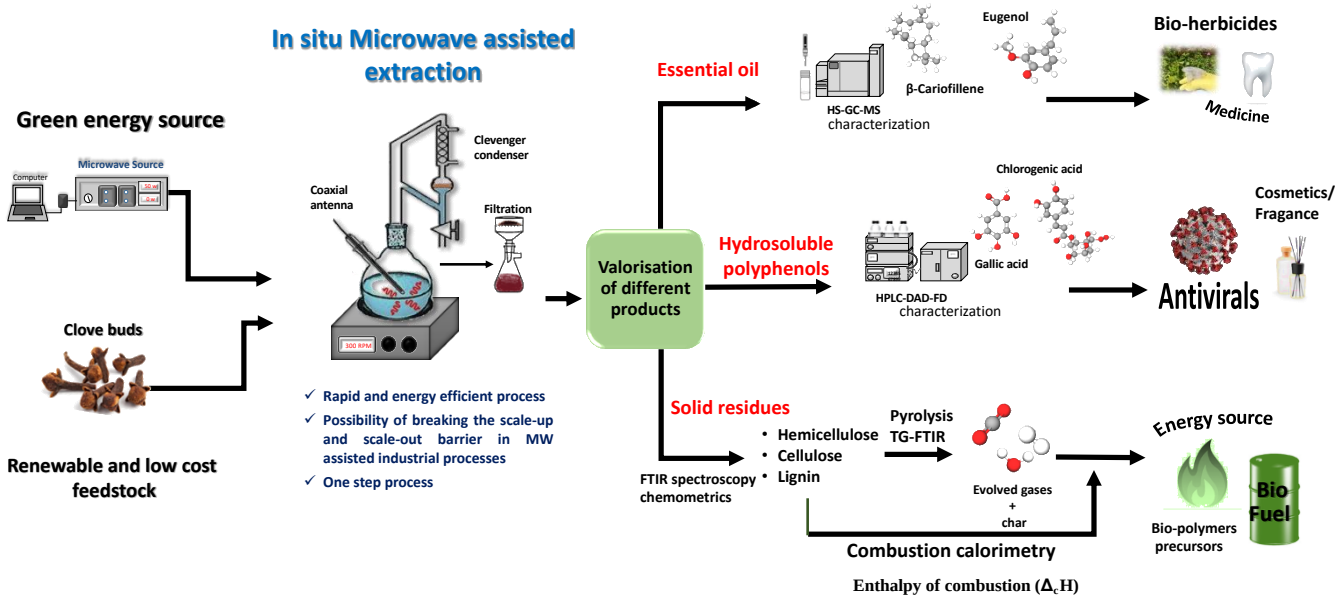

Figure 1. Overview of the herein studied approach for the isolation and characterization of different extracts from clove buds by IMWAE and its potential for biorefining. HS-GCMS=Head space gas chromatography mass spectrometry; HPLC-DAD-FD=High performance liquid chromatography with diode array detector and fluorescence detector; TG-FTIR=thermogravimetric analysis coupled to Fourier transform infrared spectroscopy; $\Delta_c H$= enthalpy of combustion.

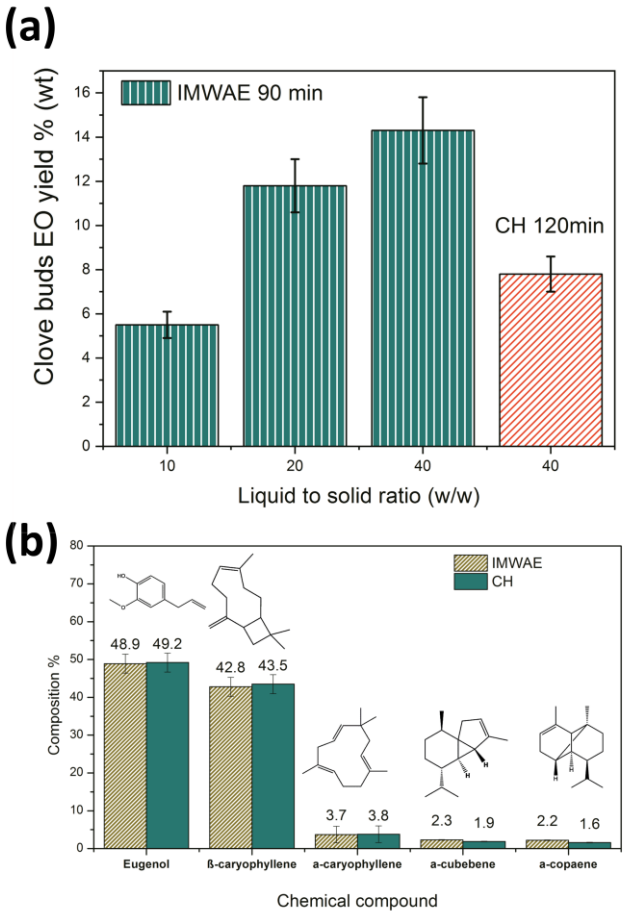

Figure 2. (a) Yield mass % of EO extracted from clove buds by IMWAE at different liquid to solid ratio. (b) Chemical composition of clove buds EO obtained by IMWAE (liquid to solid ratio=40) and CH (liquid to solid ratio=40). Extraction conditions: MW applied power 150W at 2.54 GHz, clove buds from Indonesia and water as solvent, extraction time (90 min of IMWAE and 120 min of CH, N=3 replicates). IMWAE= In situ microwave assisted extraction; CH=hydrodistillation; EO=essential oil.

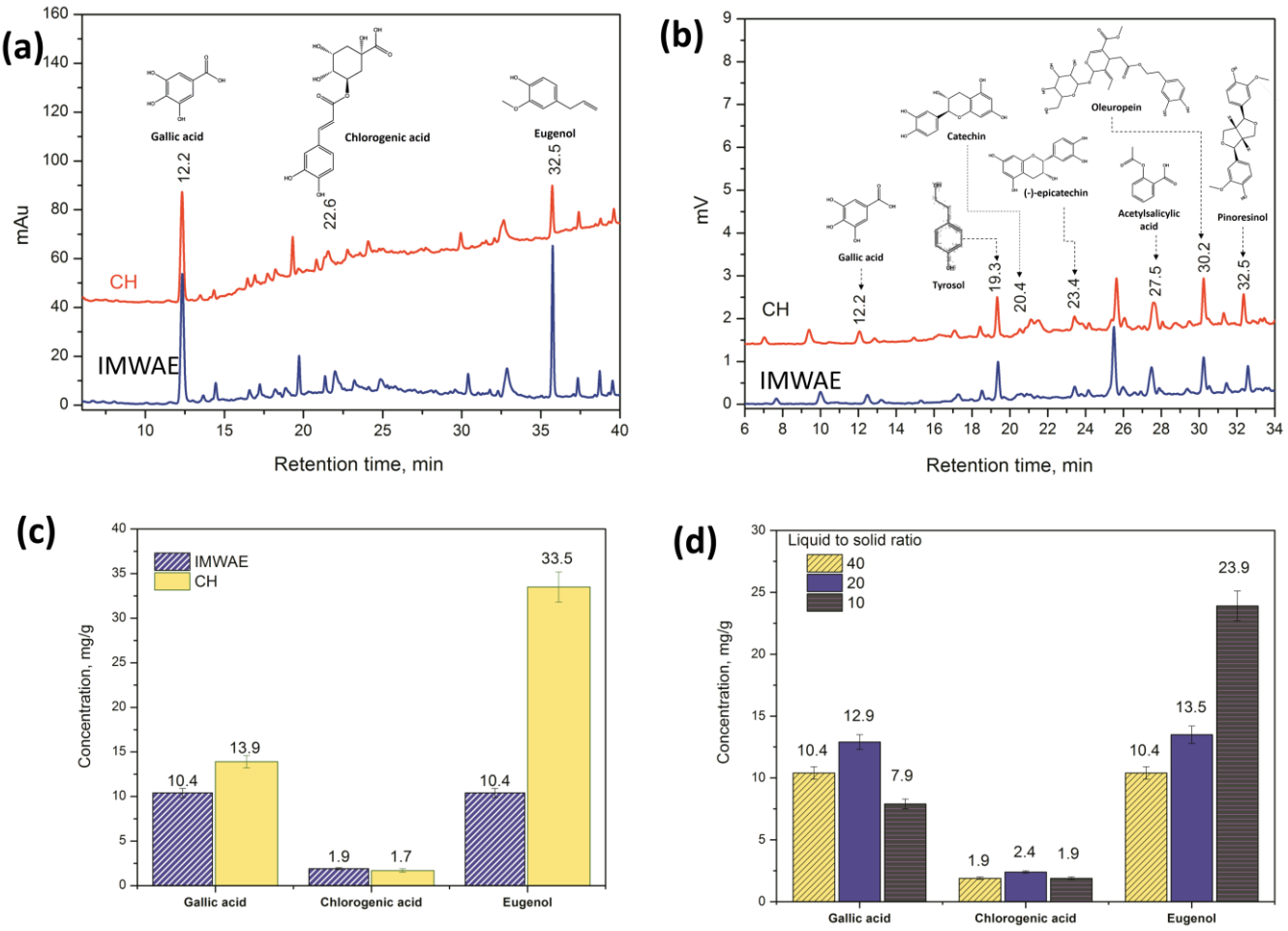

Figure 3. Polyphenols profile detected by HPLC-DAD-FD: (a) absorbance chromatogram at 280 nm, (b) fluorescence chromatogram of clove buds condensed water from IMWAE (blue line) and CH (red line) and (c) the main hydrosoluble polyphenols simultaneously quantified in condensed water after the extraction of EO from clove buds by IMWAE and CH. (d) Effect of clove bud amount (L/S_{ratio}) during IMWAE. Extraction conditions: 90 min of MW irradiation at 2.54 GHz. IMWAE= In situ microwave assisted extraction; CH=hydrodistillation; EO=essential oil.

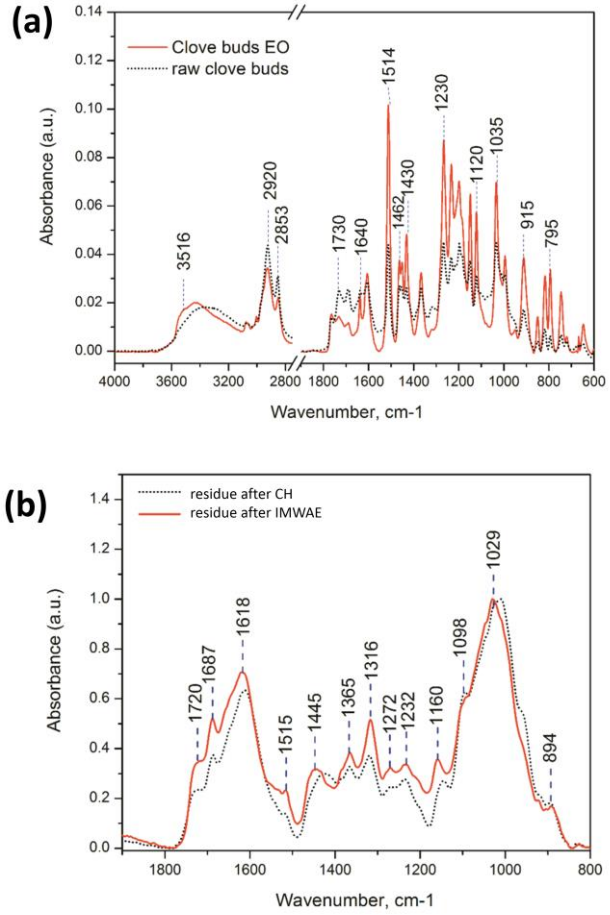

Figure 4. (a) ATR-FTIR spectra of clove buds EO and the raw clove buds. (b) ATR-FTIR spectra of the solid residue after IMWAE and CH. IMWAE= In situ microwave assisted extraction; CH=hydrodistillation; EO=essential oil.

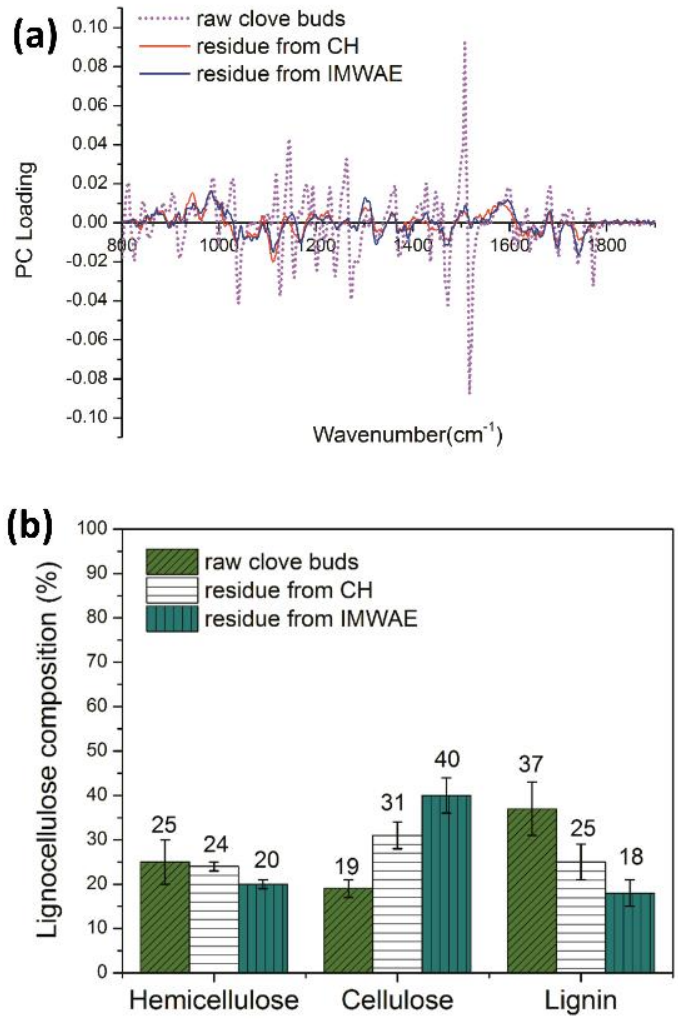

Figure 5. (a) Loadings profile (first derivative) of solid residue for the cross-validation-PLS prediction model. (b) PLS predicted chemical composition of cellulose, hemicellulose and lignin in dry solid residue after the IMWAE and CH (N= 3 replicates). IMWAE= In situ microwave assisted extraction; CH=hydrodistillation.

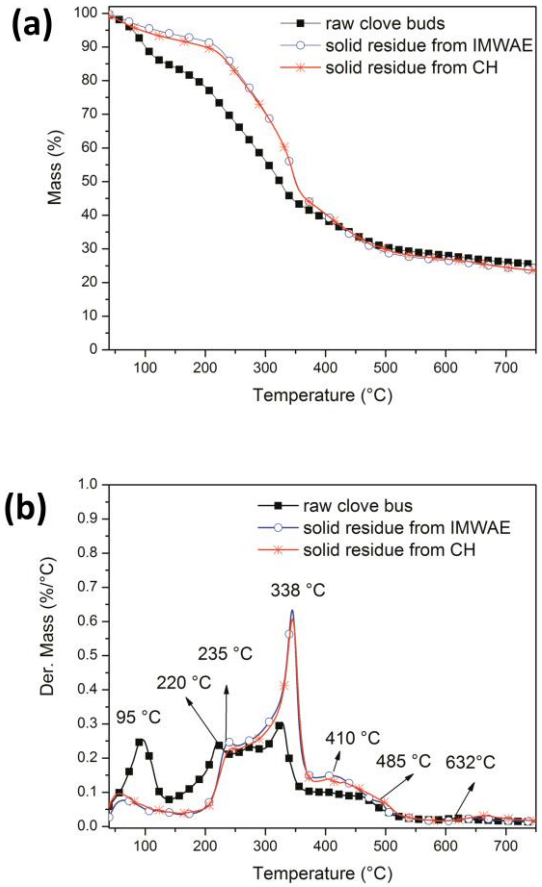

Figure 6. TG curves (a) and DTG curves (b) under nitrogen flow for the raw clove buds and solid residues from IMWAE and CH extractions. IMWAE= In situ microwave assisted extraction; CH=hydrodistillation; EO=essential oil.

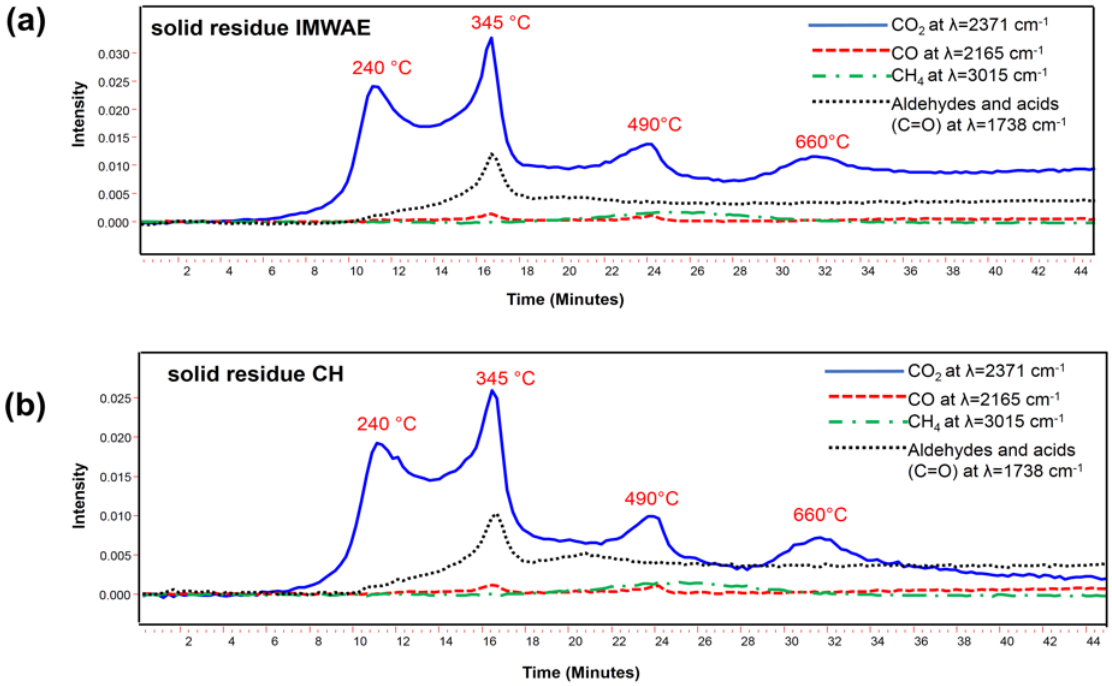

Figure 7. Evolution profiles of gases evolved from the TG-FTIR analysis of clove bud solid residues after IMWAE (a) and CH (b) (thermal decomposition at 20 °C min under N_2). IMWAE= In situ microwave assisted extraction; CH=hydrodistillation; EO=essential oil.